© 2022. Published by The Company of Biologists Ltd | Journal of Experimental Biology (2022) 225, jeb244145. doi:10.1242/jeb.244145

RESEARCH ARTICLE

Activation of p53 in anoxic freshwater crayfish, *Faxonius virilis*

Aakriti Gupta*, Sarah A. Breedon* and Kenneth B. Storey‡

ABSTRACT

Tumor suppressing transcription factor p53 regulates multiple pathways including DNA repair, cell survival, apoptosis and autophagy. Here, we studied the stress-induced activation of p53 in anoxic crayfish (*Faxonius virilis*). Relative levels of target proteins and mRNAs involved in the DNA damage response were measured in normoxic control and anoxic hepatopancreas and tail muscle. Phosphorylation levels of p53 were assessed using immunoblotting at sites known to be phosphorylated (serine 15 and 37) in response to DNA damage or reduced oxygen signaling. The capacity for DNA binding by phosphorylated p53 (p-p53) was also measured, followed by transcript analysis of a potentially pro-apoptotic downstream target, the etoposide induced (*ei24*) gene. Following this, both inhibitor (MDM2) and activator (p19-ARF) protein levels in response to low-oxygen stress were studied. The results showed an increase in p-p53 levels during anoxia in both hepatopancreas and tail muscle. Increased transcript levels of *ei24* support the activation of p53 under anoxic stress. Cytoplasmic accumulation of Ser15 phosphorylated p53 was observed during anoxia when proteins from cytoplasmic and nuclear fractions were measured. Increased cytoplasmic concentration is known to initiate an apoptotic response, which can be assumed as a preparatory step to prevent autophagy. The results suggest that p53 might play a protective role in crayfish defense against low-oxygen stress. Understanding how anoxia-tolerant organisms are able to protect themselves against DNA damage could provide important clues towards survival under metabolic rate depression and preparation for recovery to minimize damage.

KEY WORDS: Anoxia, Metabolic rate depression, Crayfish, DNA damage, Apoptosis, Stress tolerance

INTRODUCTION

Northern crayfish (*Faxonius virilis*) are a species of freshwater invertebrates native to North America, where they live at the rocky bottoms of streams (Taylor and Schuster, 2004; Taylor et al., 2007). High pollution and eutrophication in streams or stagnant pools cause severe oxygen depletion. Additionally, during winter, ponds and streams become ice-locked, limiting oxygen transfer and eventually causing decreased oxygen levels. Unlike other crustaceans that move to the surface or leave the water to breathe, *F. virilis* has a well-developed anoxia tolerance that enables these organisms to endure severe oxygen deprivation (Morris and Callaghan, 1998).

Department of Biology, Carleton University, Ottawa, ON, Canada, K1S 5B6.
*Equal co-authorship

‡Author for correspondence (kenstorey@cunet.carleton.ca)

A.G., 0000-0001-6060-9457; S.A.B., 0000-0002-6235-4045; K.B.S., 0000-0002-7363-1853

Received 17 February 2022; Accepted 12 May 2022

Several survival strategies both physical and molecular have been studied that are adopted by crayfish in response to oxygen depletion (Broughton et al., 2017; Gorr et al., 2010; McMahon, 2001). Studies have shown that under oxygen-deprived conditions, comparable species drop their metabolic rate by approximately 90% (Storey and Storey, 1990). Anoxia tolerance relies on a coordinated regulation between the activation of pro-survival and protective pathways and the suppression of non-essential functions for efficient use of the limited amount of energy available. Cell death pathways such as autophagy and apoptosis need to be prevented to extend viability. The importance of this over the period of months during which the animal is living in a hypometabolic and energy-restricted state can be appreciated. A critical decision on the maintenance or sacrifice of cells must be made for the survival of the organism.

The tumor suppressor protein p53 is a key transcription factor that regulates apoptosis, cell cycle checkpoints, cellular senescence and DNA repair, in response to stress stimuli such as DNA damage, nutrient deprivation and low-oxygen conditions, among others (Aubrey et al., 2018; Pitolli et al., 2019; Sionov and Haupt, 1999). The cellular mechanisms in response to hypoxia/anoxia have not been significantly investigated in invertebrates, but have been extensively studied in several vertebrate models under various stresses. Felix-Portillo et al. (2016) found the initiation of apoptosis during hypoxia in shrimps, independent of p53 and metallothionein. Nevertheless, in mice, p53 suppresses growth by regulating the transcription of numerous target genes. Under normal cellular conditions, p53 is ubiquitinated by the negative regulator E3 ubiquitin–protein ligase MDM2/MDM4 complex, and is maintained at low levels (Brooks and Gu, 2006; Wu and Prives, 2018). In response to stress signaling, p53 undergoes post-translational phosphorylation, and is released from the MDM2/MDM4 complex, freeing it for translocation into the nucleus (Fig. 1). In the nucleus, p53 binds to the DNA sequence in the promoter region of stress-specific genes and regulates their expression to promote either apoptosis or cell cycle arrest.

During DNA damage, amongst the multiple signaling cascades that are initiated, phosphorylation is a critical step for the stability of p53 (Fig. 1). Hyperproliferative signals activate p19-ARF, which blocks the nucleocytoplasmic shuttling of MDM2 and sequesters it to nucleoli (Weber et al., 1999). This inhibits the function of MDM2, hence preventing the degradation of p53. Activation and stabilization of p53 are further mediated under genotoxic stress by ataxia telangiectasia and Rad3-related protein (ATR) and ataxia telangiectasia mutated protein (ATM) via their substrate checkpoint kinase 1 (Chk1) and Chk2 (Pauklin et al., 2005). Chk1 and Chk2 phosphorylate serine residues S37 and S15 on p53, which prevents it from binding to MDM2, improving its function and stability (Murphy and Levine, 1998). This is considered the first step in the p53 activation process (Pauklin et al., 2005). Translocation of phosphorylated p52 (p-p53) to the nucleus regulates gene activity, contributing to cellular activities.

Journal of Experimental Biology (2022) 225, jeb244145. doi:10.1242/jeb.244145

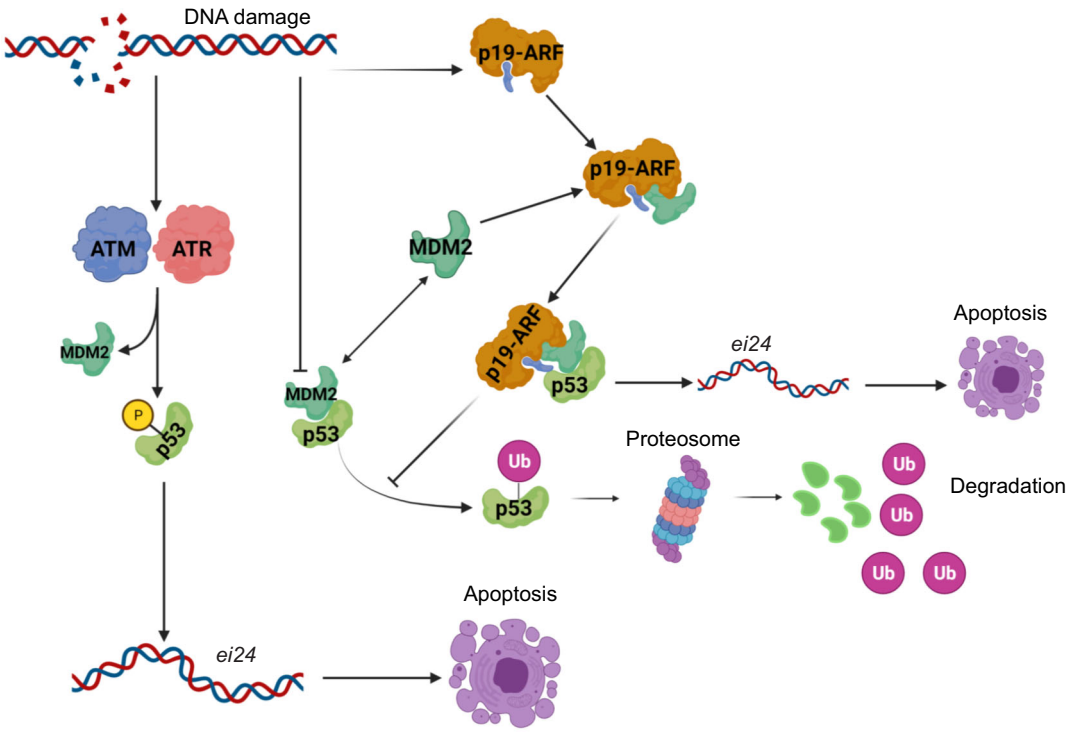

Fig. 1. An overview of the p53 DNA damage response pathway. Upon sensing DNA damage, p53 is activated via two mechanisms: (1) phosphorylation of p53 on Ser15 or Ser37 by ATM and ATR, causing p53 to disassociate from MDM2, and (2) binding of p19-ARF to the p53/MDM2 complex, preventing the degradation of p53 via proteasomal activity and resulting in the activation and stabilization of p53. Activated p53 is then free to bind to the promoter region of target genes, including *ei24*, in response to DNA damage, leading to stress-responsive apoptosis as seen in the current study. Ub, ubiquitin. Created with BioRender (biorender.com).

Etoposide-induced 2.4 kb transcript (*ei24*) – also known as p53-induced gene 8 (*PIG8*) – is highly induced by p53 in response to DNA damage. Overexpression of this gene induces apoptosis and suppresses cell growth.

DNA damage is one of the risks for organisms exposed to low-oxygen conditions. Studies have shown that hypoxia induces a cascade of signaling reactions, particularly ATM- and ATR-dependent signaling pathway, and activates Chk2 to protect cells against apoptosis and DNA damage (Blackford and Jackson, 2017; Hammond et al., 2004). Additionally, hypoxia also induces DNA-dependent protein kinase activation that induces the repair of double stranded breaks through the non-homologous end joining pathway (Bouquet et al., 2011). Considering that p53 is activated in response to fluctuations in environmental oxygen levels and that it plays an important role in preventing DNA damage, studying the p53 signaling pathway and its activation via ARF/ATM/ATR kinases is important. The current study explored the regulation the p53 DNA damage response in the tail muscle and hepatopancreas of normoxic and anoxic crayfish.

MATERIALS AND METHODS

Animal treatments

The freshwater crayfish, *Faxonius virilis* (Hagen 1870), were bought from Britannia Bait (Ottawa, ON, Canada). The crayfish were acclimatized at 15°C for 7 days prior to experimentation in aerated freshwater. The water for the crayfish in the control group was aerated with oxygen using a bubbler, whereas the water for the anoxic condition group was bubbled with 100% nitrogen gas to deoxygenate the water and induce acute anoxia. For this experiment, oxygen levels in the anoxic water were less than 1% O_2/2 Torr following 1 h of nitrogen gas bubbling. After 1 h of aerated water treatment, the control crayfish were sampled, while the crayfish for anoxic conditions were sampled after 20 h of exposure to deoxygenated water. The animal was killed via rapid decapitation and all relevant organs were flash frozen in liquid nitrogen and stored at −80°C until further use.

Total protein extraction

Total protein extracts from hepatopancreas and tail muscle tissues for control and 20 h anoxic crayfish were prepared as previously described (Gupta and Storey, 2020). Briefly, the samples were crushed in liquid nitrogen and mixed with chilled homogenization buffer (20 mmol l^{-1} Hepes, pH 7.5, 200 mmol l^{-1} NaCl, 0.1 mmol l^{-1} EDTA, 10 mmol l^{-1} NaF, 1 mmol l^{-1} Na_3VO_4 and 10 mmol l^{-1} β-glycerophosphate), 1 µl of protease inhibitor cocktail (BioShop, Burlington, ON, Canada, cat. no. PIC001.1), and a few PMSF crystals. Samples were immediately homogenized using a polytron PT10 homogenizer (Kinematica) for about 20 s and later centrifuged for 15 min at 10,000 ***g*** at 4°C. The supernatant containing total proteins was collected and the pellet was discarded. The protein concentration of the collected samples were determined using the Coomassie method with Bio-Rad prepared reagent (BioRad Laboratories, Hercules, CA, USA, cat no. 500-0006). The samples were standardized to 10 µg $µl^{-1}$ using homogenization buffer. An equal volume of 2× sodium dodecyl sulphate (SDS) buffer (100 mmol l^{-1} Tris-HCl, 20% v/v glycerol, 4% w/v SDS, 0.2% w/v Bromophenol Blue and 10% v/v β-mercaptoethanol) was added to make a working concentration of 5 µg $µl^{-1}$. The samples were boiled for 10 min and immediately chilled on ice for 10 min, then stored at −80°C until further use.

Journal of Experimental Biology

Journal of Experimental Biology (2022) 225, jeb244145. doi:10.1242/jeb.244145

Cytoplasmic and nuclear protein extraction

Frozen samples of hepatopancreas and tail muscle were weighed and ∼75 mg of each was placed in tubes pre-chilled in liquid nitrogen (n=4 biological replicates). Samples were homogenized 1:5 w/v in cytoplasmic homogenization buffer A (10 mmol l^{-1} Hepes, pH 7.9, 10 mmol l^{-1} KCl, 10 mmol l^{-1} EDTA and 20 mmol l^{-1} β-glycerophosphate) with 10 µl of 100 mmol l^{-1} dithiothreitol (DTT) and 10 µl of Protease Inhibitor Cocktail (BioShop, cat. no. P1Coo1.1) added per ml. Homogenization was performed using a Dounce homogenizer. Samples were incubated on ice for 25 min and then centrifuged at 12,000 ***g*** for 15 min at 4°C. The supernatant was transferred to new pre-chilled tubes and stored as the cytoplasmic fraction.

The pellets were re-suspended 1:5 w/v (based on original sample weights) in cytoplasmic homogenization buffer B (100 mmol l^{-1} Hepes, 2 mol l^{-1} NaCl, 5 mmol l^{-1} EDTA, 50% v/v glycerol, 100 mmol l^{-1} β-glycerophosphate, pH 7.9, and 100 mmol l^{-1} DTT) and protease inhibitor cocktail at 1:1000. The samples were sonicated using a Polytron PT1000 homogenizer (Brinkmann Instruments, Rexdale, ON, Canada) at 50% of full power for 5 s and then incubated on ice for 10 min followed by centrifugation at 14,000 ***g*** for 15 min at 4°C. The supernatant obtained was transferred to new pre-chilled tubes and stored as the nuclear fraction.

Protein concentrations in both cytoplasmic and nuclear supernatants were measured and standardized to 5 µg $µl^{-1}$ following the aforementioned procedure. Protein sample integrity and purity were checked by running both fractions on SDS-PAGE gels each with equal concentrations of cytoplasmic and corresponding nuclear fractions. The proteins were transferred to polyvinylidene difluoride (PVDF) membranes (Millipore, Etobicoke, ON, Canada, cat. no. IPVH07850, 45 µm pore). The membranes were probed with anti-histone H3 (Cell Signaling, Dancers, MA, USA, cat. no. 9715) and alpha-tubulin antibody (Santa Cruz Biotechnology, Santa Cruz, CA, USA). Histone H3 served as the nuclear marker and alpha-tubulin as the cytoplasmic marker.

SDS-PAGE and western blotting

The samples were run as previously described (Gupta and Storey, 2020). Briefly, 10%, 12% or 15% SDS PAGE resolving gels, depending on the molecular weight of the protein of interest, with 5% stacking gels were used. PiNK Plus Prestained Protein Ladder (Froggabio, cat no. PM005-0500) was used as the ladder in the first lane and 20 µg of each of the sample protein (aerobic control condition and 20 h anoxic condition) was loaded in the following lanes. A positive control sample from a mammalian species (*Ictidomys tridecemlineatus*) was run alongside the crayfish samples to confirm the appropriate band on interest. The gels were run at 180 V. Proteins were transferred to PVDF membrane by electroblotting in 1× transfer buffer (25 mmol l^{-1} Tris pH 8.5, 192 mmol l^{-1} glycine, 20% methanol) at 160 A for 90 min. Blocking was done using 3% milk w/v in TBST (20 mmol l^{-1} Tris base, pH 7.6, 140 mmol l^{-1} NaCl, 0.05% v/v Tween-20) for 30 min. Membranes were washed and incubated overnight at 4°C with protein-specific polyclonal primary antibody. The antibodies for p53 (cat. no. 2524), phospho-p53 (Ser15) (cat. no. 9284), phospho-p53 (S37) (cat. no. 9289) and p19-ARF (cat. no. 77184) were purchased from Cell Signaling (Danvers, MA, USA). The antibodies for ATM (cat. no. A01222) and ATR (cat. no. A01253) were purchased from Genscript (Piscataway, NJ, USA), and the MDM2 antibody (cat. no. SC-7918) was purchased from Santa Cruz Biotechnology (Santa Cruz, CA, USA). As *F. virilis* has not yet been sequenced, protein sequence alignments were performed with several species (*Homo sapiens*, *Mus musculus*, *I. tridecemlineatus*, *Xenopus laevis*, *Daphnia pulex*, *Penaeus vannamei* and *Drosophila melanogaster*) to ensure that the antibody epitope was conserved amongst different species. Next, the membranes were washed 3×5 min in TBST and incubated with primary antibody-specific HRP-linked secondary antibody for 30 min. The secondary antibody used in the current study was anti-rabbit IgG secondary antibody conjugated with horseradish peroxidase (cat. no. APA007P.2, BioShop). Membranes were visualized using hydrogen peroxide and luminol.

Total protein extraction for TF ELISA

The total proteins were extracted from frozen tissues of tail muscle and hepatopancreas (control and 20 h anoxia) as previously described for use in a transcription factor binding ELISA (TF ELISA) (Gupta and Storey, 2020). Briefly, a pre-chilled lysis buffer cocktail and protease inhibitor (BioShop, cat. no. PIC001) were mixed with the frozen tissue samples and homogenized using a homogenizer. The samples were then incubated on ice for 30 min and then centrifuged at 14,000 ***g*** for 20 min at 4°C. The supernatant was collected and stored at −80°C until further use. The protein concentration as measured using the Bio-Rad assay as mentioned above and protein integrity was checked by running samples on SDS-PAGE gels.

DNA binding activity using TF ELISA

Biotin labelled oligonucleotides were used for p53. The sequence of the biotin-conjugated probe was 5′-Biotin-TACCCGG-GCATGTCTAAGCATGCTG-3′, and the complementary sequence was 5′-CAGCATGCTTAGACATGCCCGGGTA-3′. Considering that p53 is a highly conserved protein, DNA–protein binding ELISAs and EMSAs conducted on other animals were referred to find the DNA binding site of p53 as used in the current experiment. A standardized protocol from previous work was followed (Gupta and Storey, 2020). Probes (biotinylated and complementary probes) were reconstituted in double distilled water to a final concentration of 500 pmol $µl^{-1}$. Forward and the reverse probes were mixed in a 1:1 ratio at 95°C for 10 min in a thermocycler. The double-stranded probes were diluted 10× to obtain a working concentration of 50 pmol $µl^{-1}$ using PBS (10 mmol l^{-1} Hepes, pH 7.9, 50 mmol l^{-1} KCl, 0.5 mmol l^{-1} EDTA, 3 mmol l^{-1} $MgCl_2$, 10% v/v glycerol, 0.5 mg ml^{-1} BSA and 0.05% NP-40); 50 µl aliquots containing 40 pmol of diluted probe were added to each well, which had been pre-coated with streptavidin (R&D Systems, Minneapolis, MB, Canada, cat. no. CA73521-134). The plate was incubated for 1 h at room temperature of 20–22°C. Aliquots of protein extracts containing 20 µg of protein were combined with 50 µl of 1× protein binding buffer [PBS, 1 µg salmon sperm DNA (BioShop), 0.5 mmol l^{-1} DTT and 40 mmol l^{-1} NaCl]. The plate was incubated at RT with mild agitation for 75 min and then washed 4 times with wash buffer. Aliquots of 60 µl of the primary antibody for phospho-p53 (S15) (Cell Signaling, cat. no. 9284) were diluted 1:250 in PBS, then added to the wells, and the plate was incubated for 3 h. The plate was then washed as above and 60 µl of anti-rabbit IgG-HRP (Bio-Shop, cat. no. APA007P.2) diluted 1:2000 in PBS was added and incubated for 1 h. Following this, the plate was washed as above and 60 µl of tetramethylbenzidine (TMB; BioShop, cat no. TMB333.100) was added. Once color had developed, the reaction was stopped by the addition of 1 mol l^{-1} HCl and optical density

was read at 450 nm with a reference wavelength of 655 nm using a Multiskan Spectrum (Thermo Electron Corporation, Waltham, MA, USA).

RNA isolation and cDNA synthesis

RNA was isolated from frozen samples of hepatopancreas and tail muscle tissues for control and 20 h anoxia-exposed crayfish; 50 mg of the samples was homogenized in 1 ml Trizol (BioShop, cat. no. TRI118.100) using a polytron PT10 homogenizer. cDNA synthesis was carried out on the samples using the protocol outlined in our previous study (Gupta and Storey, 2021a).

Primer design and RT-qPCR

Forward and reverse primers for *ei24* were designed from conserved regions based on DNA alignment of the sequences from both vertebrate and invertebrate species for use in quantitative reverse transcription PCR (RT-qPCR). Primers were designed using Primer Blast by the National Center for Biotechnology Information (NCBI; https://www.ncbi.nlm.nih.gov/tools/primer-blast/). Primers used for *ei24* and *tubulin* (control) were as follows: *tubulin* forward 5′ GACATTTGTTCATGGTATGC 3′, reverse 5′ TGTCGGTG-GAATAGGGAAAG 3′; *ei24* forward 5′ TATAGCATGTG-CACTGTGCC 3′, reverse 5′ GTCTGTACTCCGGGAACAAC 3′. The PCR program consisted of 7 min at 94°C, followed by 35 cycles of 1 min at 94°C, 1 min at 58°C for *ei24* and 53°C for *tubulin*, and 1.5 min at 72°C. The final step was 72°C for 10 min. PCR products were separated on a 1% agarose gel stained with ethidium bromide, visualized using the ChemiGenius imaging system (Syngene, Frederick, MD, USA) under UV light and quantified using the GeneTools program. The bands from the most dilute cDNA sample that gave visible product were used for quantification to ensure that the products had not reached amplification saturation. PCR products were sequenced by DNA Landmarks (Saint-Jean-sur-Richelieu, QC, Canada) and sequences were verified as encoding the correct genes using the program BLASTN (http://www.ncbi.nlm.nih.gov/blast).

Data analysis and statistics

Immunoblot protein bands were quantified by densitometric analysis using ChemiGenius BioImaging System and the associated GeneTools software (Syngene). To control for irregularities in SDS-PAGE gel loading, band intensity in each lane was normalized against the corresponding density of Coomassie-stained protein bands in the same lane. Immunoblot data for each condition are expressed as means±s.e.m., with n=4 samples from different animals. Statistical analysis used one-way ANOVA, with Dunnett's *post hoc* test, using the RBioPlot software, with $P<0.05$ accepted as significant (Zhang and Storey, 2016).

RESULTS

Effect of anoxia on p53 protein expression and phosphorylation

Relative protein levels of p53 were detected using immunoblotting and a single band around 53 kDa was observed in both hepatopancreas and tail muscle. The results showed no change in the protein levels of p53 in both hepatopancreas and tail muscle under anoxic conditions when compared with control (Fig. 2). The levels of Ser37 phosphorylated p53 (p-p53 S37) were measured using a polyclonal anti-p-p53 S37-specific antibody. It was observed that levels in the hepatopancreas significantly increased by 1.4(±0.05)-fold in anoxic conditions and by 1.71(±0.12)-fold in anoxic tail muscle relative to control levels (Fig. 2).

Effect of anoxia on ATM and ATR protein expression

Changes in the levels of ATM and ATR were observed in response to anoxia. Relative levels of ATM increased significantly during anoxia in both hepatopancreas and tail muscle by 3.07(±0.31)-fold and 1.33(±0.02)-fold, respectively, relative to control (Fig. 2). Similarly, a significant increase was observed in protein levels of ATR during anoxia in both tissues; in the hepatopancreas, levels increased by 2.37(±0.19)-fold relative to control, and in tail muscle, an increase of 1.49(±0.14)-fold relative to control was observed (Fig. 2).

Effect of anoxia on p19-ARF and MDM2 protein expression

In response to low oxygen levels, p19-ARF acts as an activator and MDM2 acts as an inhibitor to p53. Therefore, relative protein levels of both activator and inhibitor were measured. Under anoxic conditions, there was a significant increase of 1.95(±0.25)-fold in p19-ARF expression relative to control in the hepatopancreas, and a 1.22(±0.02)-fold increase relative to control in tail muscle (Fig. 2). The level of MDM2 decreased significantly during anoxia to 57.2±9.2% compared with control in hepatopancreas, and 59.4±6.4% compared with control in tail muscle (Fig. 2).

Relative protein levels and cellular localization of p-p53 S15

Upon phosphorylation at Ser15, p53 detaches from MDM2 and translocates to the nucleus, resulting in stress-specific transcriptional activation of numerous genes. Therefore, along with the total cellular protein expression changes in p-p53 S15, the protein levels in cytoplasmic and nuclear fractions were also assessed. The phosphorylation profile in hepatopancreas total protein levels showed a significant increase in p-p53 S15 by 1.95(±0.26)-fold during anoxia relative to control values, whereas no significant change was observed in anoxic tail muscle (Fig. 2). Cytoplasmic levels of p-p53 S15 showed a significant increase during anoxia in both tissues relative to control – 2.15(±0.11)-fold in hepatopancreas and 1.50(±0.10)-fold in tail muscle – but no significant change was observed in nuclear protein expression for either tissue (Fig. 3).

DNA binding activity of p53 in response to anoxia

In response to anoxia, changes in the DNA binding activity of p-p53 S15 were assessed using a TF ELISA. The results showed a significant decrease in the binding levels of p-p53 S15 during anoxia to 38±6% compared with control levels in the hepatopancreas, whereas a significant increase of 2.23(±0.23)-fold relative to control was observed in anoxic tail muscle (Fig. 4).

Transcript levels of *ei24* in response to anoxia

ei24 is one of the downstream targets of p53 that is linked with apoptosis. Changes in the transcript levels of *ei24* in response to anoxia were measured using RT-qPCR. No significant change was observed in the mRNA levels of the gene in anoxic hepatopancreas, while *ei24* transcript levels increased significantly by 1.80(±0.02)-fold relative to control in anoxic tail muscle (Fig. 5).

DISCUSSION

Many organisms encounter environmental stress in their natural habitats brought on by seasonal temperature changes (desiccation in high temperatures, freezing in low temperatures), changes in oxygen levels (hypoxia/anoxia), or a drop in nutrient availability (caloric restriction) (Storey, 2015; Storey and Storey, 1990). Many organisms adopt a similar strategy to survive hypoxic and anoxic conditions in their regular stages of life, including turtles (Breedon

Journal of Experimental Biology (2022) 225, jeb244145. doi:10.1242/jeb.244145

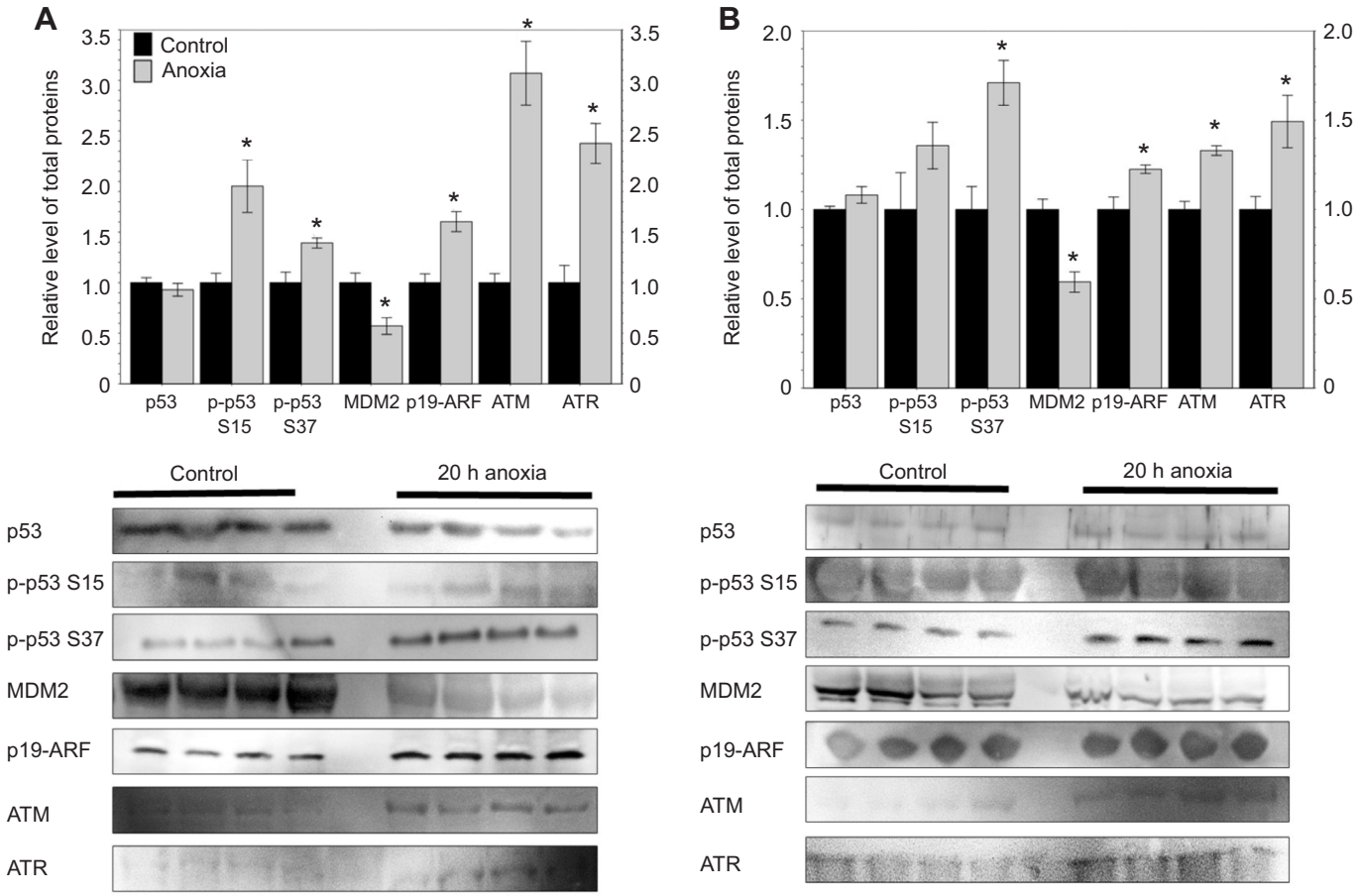

Fig. 2. Effect of anoxia on protein expression and phosphorylation. Relative protein expression of p53, phosphorylated p53 (p-p53 S15 and S37), the p53 inhibitor (MDM2) and p53 activators (ATM, ATR, p19-ARF) in (A) hepatopancreas and (B) tail muscle of crayfish in normoxic control and 20 h anoxic conditions as determined by western immunoblotting. Corresponding western immunoblots are shown below histograms. Data are expressed as means±s.e.m., n=3–4 independent samples from different animals. Data were analyzed using a two-tailed Student's t-test, with *P<0.05 considered as statistically significant.

et al., 2021; Gupta et al., 2021b), brine shrimp (Storey and Storey, 2011), crayfish (English et al., 2018; Green and Storey, 2016) and wood frogs (Gupta and Storey, 2021b, 2022; Gupta et al., 2020; Wu et al., 2018), among many others (Gupta et al., 2021a; Krivoruchko and Storey, 2010; Tessier et al., 2017). Many stress-tolerant organisms undergo metabolic rate depression (MRD), entering a hypometabolic state and reprioritizing their energy expenditure to favor pro-survival pathways (Gupta et al., 2021b; Storey, 1998, 2004; Storey and Storey, 2005), including DNA damage repair. The northern crayfish is a good model for studying hypometabolism during anoxic conditions, allowing us to examine how they regulate p53 to circumvent apoptosis and promote DNA repair to sustain long-term viability under anoxic conditions.

ATM and ATR kinases respond to DNA breaks at different checkpoints via different stimuli; double-stranded breaks in DNA trigger ATM (Bakkenist and Kastan, 2003), whereas UV damage/stalled replication forks trigger ATR (Zou and Elledge, 2003). Interestingly, both proteins are activated during hypoxia and reoxygenation (Fallone et al., 2013; Hammond and Giaccia, 2004; Olcina et al., 2014). ATR is activated as a result of S-phase arrest during hypoxia (Fallone et al., 2013), while ATM can be activated via non-DNA damaging signals during hypoxia and by increased reactive oxygen species (ROS) during reoxygenation (Olcina et al., 2014). Therefore, we would expect to see increased expression of both proteins during anoxia, which was indeed observed, with a significant increase in both ATM and ATR in anoxic hepatopancreas and tail muscle relative to control values (Fig. 2), confirming the oxygen sensitivity of crayfish.

p53 is a nuclear phosphoprotein that responds to environmental stress, specifically low oxygen levels and genomic damage, under tight regulation. As such, the relative expression of total cellular protein was analyzed. Interestingly, no significant change was observed during anoxia in either the hepatopancreas or tail muscle (Fig. 2). A likely explanation for this observation is that p53 undergoes significant post-translational modifications in response to stress signaling/genomic damage, without significantly changing its overall cellular concentration, corresponding to our findings of increased ATM and ATR protein expression. Studies have reported that p53 is activated by post-translational modifications, including phosphorylation, acetylation and glycosylation, in a stress-specific manner (Ko and Prives, 1996). Upon sensing DNA damage, p53 is phosphorylated at serine residues 15, 20, 33 and 37 in the amino-terminal domain, which plays an essential role in p53 activity and stability (Ashcroft and Vousden, 1999). Several kinases including ATM and ATR have been reported to phosphorylate p53 in a stress-specific manner (Lakin and Jackson, 1999). A study showed that even though ATR phosphorylates p53 at S15 and S37, ATM does not play any role in modification at S37 (Tibbetts et al., 1999). Hence, this study focused on phosphorylation of p53 at S15 and S37. Phosphorylation of H2A histone family member X (H2AX) is one of the initial responses to DNA damage and repair. H2AX is phosphorylated at Ser129 to become γH2AX (Mah et al., 2010).

Journal of Experimental Biology (2022) 225, jeb244145. doi:10.1242/jeb.244145

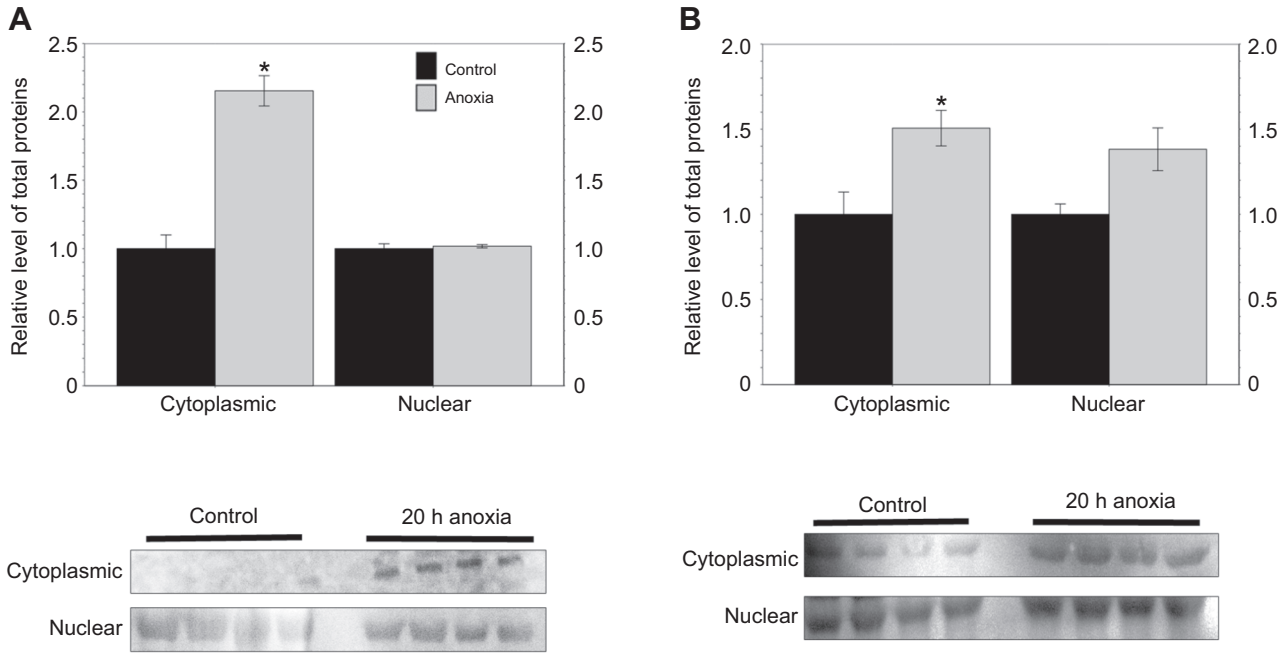

Fig. 3. Cellular localization of p-p53 S15. Relative expression levels of p-p53 S15 in cytoplasmic and nuclear fractions in (A) hepatopancreas and (B) tail muscle of crayfish in normoxic control and 20 h anoxic conditions as determined by western immunoblotting. Other information as in Fig. 2. *P<0.05.

Phosphorylation levels act as a very specific and sensitive molecular marker to detect the extent of DNA damage (Mah et al., 2010). Further research on γH2AX levels in crayfish in response to anoxia is warranted to study how crayfish minimize DNA damage during anoxia.

Phosphorylation of p53 at S15 and S37 sites stimulates transcriptional activity during cellular stress (Dohoney et al., 2004). ATM and ATR can phosphorylate p53 at S15 to enhance its transactivation activity (Banin et al., 1998). Interestingly, under anoxic conditions, p53 was activated by S15 phosphorylation in hepatopancreas, with a significant increase in p-p53 S15 during anoxic conditions compared with control, whereas no significant change was observed in the levels of p-p53 S15 in tail muscle (Fig. 2). Additionally, relative protein levels of p-p53 S15 increased significantly in the cytoplasmic fraction of both the hepatopancreas and tail muscle during anoxia. Although an increasing trend was observed in the relative levels of p-p53 S15 in the nuclear fraction of anoxic tail muscle, the change was not significant (Fig. 3).

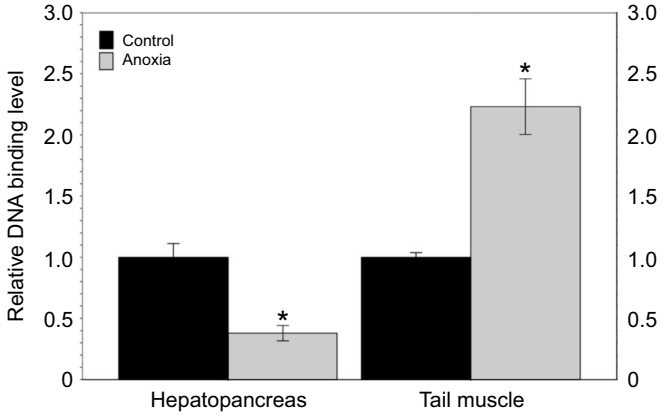

Fig. 4. Effect of anoxia on p53 DNA binding. Relative DNA binding levels of p-p53 S15 in (A) hepatopancreas and (B) tail muscle of crayfish under normoxic control and 20 h anoxic conditions as determined by transcription factor binding ELISA (TF ELISA). Other information as in Fig. 2. *P<0.05.

Enhanced cytoplasmic expression of p53 during anoxia observed in this current study in both hepatopancreas and tail muscle suggests an important role in the cytoplasm (Fig. 3). This finding is supported by studies which suggest that the build-up of p53 in the cytoplasm is essential for triggering many extracellular activities (Chipuk et al., 2004; Mihara et al., 2003). Furthermore, its abundance in cytoplasm inhibits autophagy and triggers intrinsic apoptotic machinery (Green and Kroemer, 2009). A study by Sun et al. (2016) in river prawn highlighted the same results, showing the presence of high levels of p53 in hepatopancreas compared with other tissues (Sun et al., 2016). Additionally, they observed a buildup of oxidative stress in hypoxic prawns (Sun et al., 2016). Anoxic conditions activate pro-apoptotic Bcl2 proteins, a downstream target of p53, and caspases to initiate apoptosis (Fridman and Lowe, 2003). Therefore, activation of apoptosis and inhibition of autophagy, as suggested previously, is an organized way to clear up cells damaged as a result of anoxia without harming the surrounding cells. Being an ATP-dependent process, the accumulation of p53 to initiate apoptosis could also be a preparatory mechanism for recovery (Eguchi et al., 1997). This is because, during anoxic conditions, cells are in a hypometabolic state with limited energy availability, so processes such as apoptosis could be halted until aerobic recovery.

The DNA binding activity of p-p53 S15 showed a relative increase in the level of binding in anoxic tail muscle when compared with control (Fig. 4). Therefore, increased binding of transcription factor p-p53 S15 to the promoter region of the DNA could result in increased transcript levels of genes under the regulation of p-p53 S15 in the nucleus during anoxia. The increase in the relative transcript levels of *ei24* in anoxic tail muscle corresponded with the results obtained on the DNA binding ability of p-p53 S15 (Fig. 5). The tumor suppressor gene *ei24* is a downstream target of p53 with a pro-apoptotic function to suppress cellular growth (Sung et al., 2013). This supports the presence of transcriptionally active p53 in the cells. *ei24*

Journal of Experimental Biology (2022) 225, jeb244145. doi:10.1242/jeb.244145

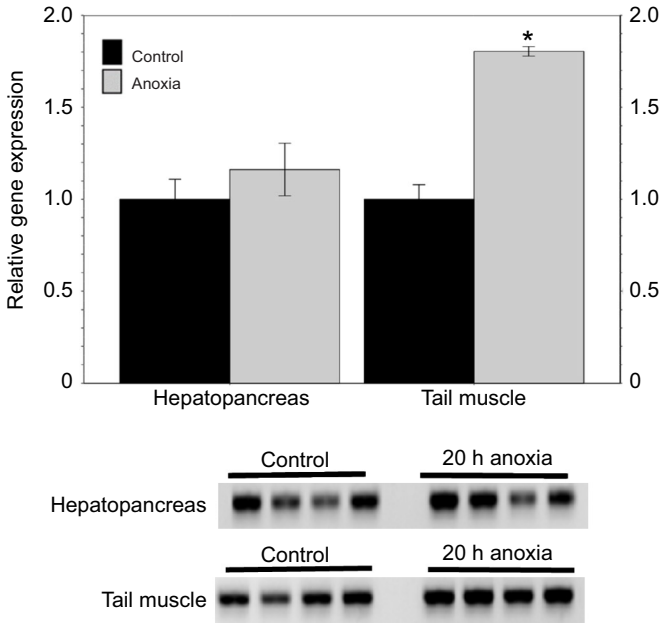

Fig. 5. Effect of anoxia on *ei24* expression. Relative transcript levels of *ei24* in (A) hepatopancreas and (B) tail muscle of crayfish under normoxic control and 20 h anoxic conditions as determined by RT-qPCR. Other information as in Fig. 2. **P*<0.05.

negatively regulates cell growth and induces apoptosis (Gentile et al., 2001; Gu et al., 2000). The increased expression of *ei24* is likely either in preparation for increased apoptosis during aerobic recovery, when ROS production would be significantly elevated as a result of the sudden influx of oxygen, or for the induction of apoptosis during anoxic conditions as a protective mechanism to prevent the spread of cytotoxins resulting from autophagy or necrosis. Future research on oxidative stress in anoxic crayfish could provide better insight into the interplay of p53 activation, apoptosis and autophagy.

Relative protein expression of p-p53 S37 showed a significant increase in both anoxic hepatopancreas and tail muscles (Fig. 2). Phosphorylation prevents the binding of p53 to MDM2, which allows accumulation and activation of p53 during DNA damage (Shieh et al., 1997; Tibbetts et al., 1999). Accumulation of p-p53 S37 further supports the increased concentration of p53 in the cytoplasm during anoxia in both tissues (Figs 2 and 3). Given the role that MDM2 plays in p53 inactivation, it is expected that in order to increase levels of activated p53, there would be a similar decrease in MDM2 expression (Ashcroft and Vousden, 1999). Indeed, MDM2 protein levels were significantly decreased in both the tissues during anoxia. Considering that the northern crayfish has not been sequenced and phosphorylation of p53 is not well studied in crustaceans, a detailed investigation and mass spectrometry analysis to find the exact phosphorylation sites would be required for confirmation of these results.

Another mechanism that stabilizes p53 involves the activation of p19-ARF during DNA damage. p19-ARF binds to MDM2 in a region that is different from the p53 binding domain. This interaction inhibits the ubiquitin ligase activity of MDM2, preventing the degradation of p53 by MDM2 without affecting the binding of p53 with MDM2 (Honda, 1999). The increased levels of p19-ARF under anoxic conditions in both tissues suggest the stabilization of p53 in response to stress (Fig. 2). Altogether, decreased MDM2 levels, increased p53 S37 phosphorylation and increased p19-ARF expression would result in increased levels of p53-mediated transcription under stress.

Conclusions

The tumor suppressor protein p53 plays a critical role in programmed cell death in response to cellular stress. p53 stability and activation is a complex mechanism that is regulated via inhibition by MDM2, and phosphorylation-mediated activation by ATM/ATR. The findings presented in the current study suggest that under anoxic conditions, p53 is activated and stabilized by increased S15 and S37 phosphorylation, increased ATM, ATR and p19-ARF levels, and decreased MDM2 levels. The stability of p53 was confirmed by the increased transcript levels of *ei24* under anoxia, an important downstream target of p53 that is transcribed in response to DNA damage. The increased protein levels of p53 and transcript levels of *ei24* suggest activation of a protective mechanism against DNA damage and autophagy during anoxia. Taken altogether, upon sensing DNA damage, p53 is activated via phosphorylation and/or by p19-ARF. p53 is then free to act in the nucleus where it can promote the transcription of *ei24*, while also accumulating in the cytoplasm as a mechanism to restrict autophagy and resulting DNA damage. Overall, the results presented herein suggest the promotion of apoptosis in contrast to autophagy, which could potentially cause deleterious cytotoxicity. The current study provides important insights into the signaling mechanism and response of p53 to DNA damage in crayfish. However, further studies focusing on the specific regulation of apoptosis and autophagy in anoxic crayfish are needed to confirm these findings.

Acknowledgements

The authors thank J. M. Storey for comments on the manuscript and B. Lant for experimental contribution.

Competing interests

The authors declare no competing or financial interests.

Author contributions

Conceptualization: A.G., S.A.B.; Methodology: A.G., S.A.B.; Software: A.G., S.A.B.; Validation: A.G., S.A.B.; Formal analysis: A.G., S.A.B.; Investigation: A.G., S.A.B.; Resources: K.B.S.; Data curation: A.G., S.A.B.; Writing - original draft: A.G.; Writing - review & editing: A.G., S.A.B.; Visualization: A.G., S.A.B.; Supervision: K.B.S.; Project administration: A.G., S.A.B.; Funding acquisition: K.B.S.

Funding

This research was supported by a Discovery grant from the Natural Sciences and Engineering Research Council of Canada (RGPIN-2020-04733); K.B.S. holds the Canada Research Chair in Molecular Physiology.

References

Ashcroft, M. and Vousden, K. H. (1999). Regulation of p53 stability. *Oncogene* **18**, 7637-7643. doi:10.1038/sj.onc.1203012

Aubrey, B. J., Kelly, G. L., Janic, A., Herold, M. J. and Strasser, A. (2018). How does p53 induce apoptosis and how does this relate to p53-mediated tumour suppression? *Cell Death Differ.* **25**, 104-113. doi:10.1038/cdd.2017.169

Bakkenist, C. J. and Kastan, M. B. (2003). DNA damage activates ATM through intermolecular autophosphorylation and dimer dissociation. *Nature* **421**, 499-506. doi:10.1038/nature01368

Banin, S., Moyal, L., Shieh, S., Taya, Y., Anderson, C. W., Chessa, L., Smorodinsky, N. I., Prives, C., Reiss, Y., Shiloh, Y. et al. (1998). Enhanced phosphorylation of p53 by ATM in response to DNA damage. *Science* **281**, 1674-1677. doi:10.1126/science.281.5383.1674

Blackford, A. N. and Jackson, S. P. (2017). ATM, ATR, and DNA-PK: the trinity at the heart of the DNA damage response. *Mol. Cell* **66**, 801-817. doi:10.1016/j.molcel.2017.05.015

Bouquet, F., Ousset, M., Biard, D., Fallone, F., Dauvillier, S., Frit, P., Salles, B. and Muller, C. (2011). A DNA-dependent stress response involving DNA-PK occurs in hypoxic cells and contributes to cellular adaptation to hypoxia. *J. Cell Sci.* **124**, 1943-1951. doi:10.1242/jcs.078030

Breedon, S. A., Hadj–Moussa, H. and Storey, K. B. (2021). Nrf2 activates antioxidant enzymes in the anoxia–tolerant red–eared slider turtle. *Trachemys scripta elegans*. *J. Exp. Zool. A Ecol. Integr. Physiol.* **335**, 426-435. doi:10.1002/jez.2458

Brooks, C. L. and Gu, W. (2006). p53 ubiquitination: Mdm2 and beyond. *Mol. Cell* **21**, 307-315. doi:10.1016/j.molcel.2006.01.020

Broughton, R. J., Marsden, I. D., Hill, J. V. and Glover, C. N. (2017). Behavioural, physiological and biochemical responses to aquatic hypoxia in the freshwater crayfish, *Paranephrops zealandicus*. *Comp. Biochem. Physiol. A Mol. Integr. Physiol.* **212**, 72-80. doi:10.1016/j.cbpa.2017.07.013

Chipuk, J. E., Kuwana, T., Bouchier-Hayes, L., Droin, N. M., Newmeyer, D. D., Schuler, M. and Green, D. R. (2004). Direct activation of bax by p53 mediates mitochondrial membrane permeabilization and apoptosis. *Science* **303**, 1010-1014. doi:10.1126/science.1092734

Dohoney, K. M., Guillerm, C., Whiteford, C., Elbi, C., Lambert, P. F., Hager, G. L. and Brady, J. N. (2004). Phosphorylation of p53 at serine 37 is important for transcriptional activity and regulation in response to DNA damage. *Oncogene* **23**, 49-57. doi:10.1038/sj.onc.1207005

Eguchi, Y., Shimizu, S. and Tsujimoto, Y. (1997). Intracellular ATP levels determine cell death fate by apoptosis or necrosis. *Cancer Res.* **57**, 1835-1840.

English, S. G., Hadj-Moussa, H. and Storey, K. B. (2018). MicroRNAs regulate survival in oxygen-deprived environments. *J. Exp. Biol.* **221**, jeb190579. doi:10.1242/jeb.190579

Fallone, F., Britton, S., Nieto, L., Salles, B. and Muller, C. (2013). ATR controls cellular adaptation to hypoxia through positive regulation of hypoxia-inducible factor 1 (HIF-1) expression. *Oncogene* **32**, 4387-4396. doi:10.1038/onc.2012.462

Felix-Portillo, M., Martínez-Quintana, J. A., Arenas-Padilla, M., Mata-Haro, V., Gómez-Jiménez, S. and Yepiz-Plascencia, G. (2016). Hypoxia drives apoptosis independently of p53 and metallothionein transcript levels in hemocytes of the whiteleg shrimp *Litopenaeus vannamei*. *Chemosphere* **161**, 454-462. doi:10.1016/j.chemosphere.2016.07.041

Fridman, J. S. and Lowe, S. W. (2003). Control of apoptosis by p53. *Oncogene* **22**, 9030-9040. doi:10.1038/sj.onc.1207116

Gentile, M., Ahnström, M., Schön, F. and Wingren, S. (2001). Candidate tumour suppressor genes at 11q23–q24 in breast cancer: evidence of alterations in PIG8, a gene involved in p53-induced apoptosis. *Oncogene* **20**, 7753-7760. doi:10.1038/sj.onc.1204993

Gorr, T. A., Wichmann, D., Hu, J., Hermes–Lima, M., Welker, A. F., Terwilliger, N., Wren, J. F., Viney, M., Morris, S., Nilsson, G. E. et al. (2010). Hypoxia tolerance in animals: biology and application. *Physiol. Biochem. Zool.* **83**, 733-752. doi:10.1086/648581

Green, D. R. and Kroemer, G. (2009). Cytoplasmic functions of the tumour suppressor p53. *Nature* **458**, 1127-1130. doi:10.1038/nature07986

Green, S. R. and Storey, K. B. (2016). Regulation of crayfish, *Orconectes virilis*, tail muscle lactate dehydrogenase (LDH) in response to anoxic conditions is associated with alterations in phosphorylation patterns. *Comp. Biochem. Physiol. B Biochem. Mol. Biol.* **202**, 67-74. doi:10.1016/j.cbpb.2016.08.004

Gu, Z., Flemington, C., Chittenden, T. and Zambetti, G. P. (2000). ei24, a p53 response gene involved in growth suppression and apoptosis. *Mol. Cell. Biol.* **20**, 233-241. doi:10.1128/MCB.20.1.233-241.2000

Gupta, A. and Storey, K. B. (2020). Regulation of antioxidant systems in response to anoxia and reoxygenation in *Rana sylvatica*. *Comp. Biochem. Physiol. B Biochem. Mol. Biol.* **243-244**, 110436. doi:10.1016/j.cbpb.2020.110436

Gupta, A. and Storey, K. B. (2021a). Coordinated expression of Jumonji and AHCY under OCT transcription factor control to regulate gene methylation in wood frogs during anoxia. *Gene* **788**, 145671. doi:10.1016/j.gene.2021.145671

Gupta, A. and Storey, K. B. (2021b). Activation of the hippo pathway in *Rana sylvatica*: yapping stops in response to anoxia. *Elife* **11**, 1422. doi:10.3390/life11121422

Gupta, A. and Storey, K. B. (2022). A "notch" in the cellular communication network in response to anoxia by wood frog (Rana sylvatica). *Cell. Signal.* **93**, 110305. doi:10.1016/j.cellsig.2022.110305

Gupta, A., Brooks, C. and Storey, K. B. (2020). Regulation of NF-κB, FHC and SOD2 in response to oxidative stress in the freeze tolerant wood frog, *Rana sylvatica*. *Cryobiology* **97**, 28-36. doi:10.1016/j.cryobiol.2020.10.012

Gupta, A., Hadj-Moussa, H., Al-attar, R., Seibel, B. A. and Storey, K. B. (2021a). Hypoxic jumbo squid activate neuronal apoptosis but not MAPK or antioxidant enzymes during oxidative stress. *Physiol. Biochem. Zool.* **94**, 171-179. doi:10.1086/714097

Gupta, A., Varma, A. and Storey, K. B. (2021b). New insights to regulation of fructose-1,6-bisphosphatase during anoxia in red-eared slider, *Trachemys scripta elegans*. *Biomolecules* **11**, 1548. doi:10.3390/biom11101548

Hammond, E. M. and Giaccia, A. J. (2004). The role of ATM and ATR in the cellular response to hypoxia and re-oxygenation. *DNA Repair* **3**, 1117-1122. doi:10.1016/j.dnarep.2004.03.035

Hammond, E. M., Dorie, M. J. and Giaccia, A. J. (2004). Inhibition of ATR leads to increased sensitivity to hypoxia/reoxygenation. *Cancer Res.* **64**, 6556-6562. doi:10.1158/0008-5472.CAN-04-1520

Honda, R. (1999). Association of p19ARF with Mdm2 inhibits ubiquitin ligase activity of Mdm2 for tumor suppressor p53. *EMBO J.* **18**, 22-27. doi:10.1093/emboj/18.1.22

Ko, L. J. and Prives, C. (1996). p53: puzzle and paradigm. *Genes Dev.* **10**, 1054-1072. doi:10.1101/gad.10.9.1054

Krivoruchko, A. and Storey, K. B. (2010). Forever young: mechanisms of natural anoxia tolerance and potential links to longevity. *Oxid. Med. Cell Longev.* **3**, 186-198. doi:10.4161/oxim.3.3.12356

Lakin, N. D. and Jackson, S. P. (1999). Regulation of p53 in response to DNA damage. *Oncogene* **18**, 7644-7655. doi:10.1038/sj.onc.1203015

Mah, L.-J., El-Osta, A. and Karagiannis, T. C. (2010). γH2AX: a sensitive molecular marker of DNA damage and repair. *Leukemia* **24**, 679-686. doi:10.1038/leu.2010.6

McMahon, B. R. (2001). Respiratory and circulatory compensation to hypoxia in crustaceans. *Respir. Physiol.* **128**, 349-364. doi:10.1016/S0034-5687(01)00311-5

Mihara, M., Erster, S., Zaika, A., Petrenko, O., Chittenden, T., Pancoska, P. and Moll, U. M. (2003). p53 has a direct apoptogenic role at the mitochondria. *Mol. Cell* **11**, 577-590. doi:10.1016/S1097-2765(03)00050-9

Morris, S. and Callaghan, J. (1998). The emersion response of the Australian Yabby Cherax destructor to environmental hypoxia and the respiratory and metabolic responses to consequent air-breathing. *J. Comp. Physiol. B Biochem. Syst. Environ. Physiol.* **168**, 389-398. doi:10.1007/s003600050158

Murphy, M. and Levine, A. J. (1998). The role of p53 in apoptosis. In *Apoptosis Genes* (ed. J. W. Wilson, C. Booth, C. S. Potten), pp. 5-35. Boston: Springer.

Olcina, M. M., Grand, R. J. A. and Hammond, E. M. (2014). ATM activation in hypoxia - causes and consequences. *Mol. Cell. Oncol.* **1**, e29903. doi:10.4161/mco.29903

Pauklin, S., Kristjuhan, A., Maimets, T. and Jaks, V. (2005). ARF and ATM/ATR cooperate in p53-mediated apoptosis upon oncogenic stress. *Biochem. Biophys. Res. Commun.* **334**, 386-394. doi:10.1016/j.bbrc.2005.06.097

Pitolli, C., Wang, Y., Candi, E., Shi, Y., Melino, G. and Amelio, I. (2019). p53-mediated tumor suppression: DNA-damage response and alternative mechanisms. *Cancers* **11**, 1983. doi:10.3390/cancers11121983

Shieh, S.-Y., Ikeda, M., Taya, Y. and Prives, C. (1997). DNA damage-induced phosphorylation of p53 alleviates inhibition by MDM2. *Cell* **91**, 325-334. doi:10.1016/S0092-8674(00)80416-X

Sionov, R. V. and Haupt, Y. (1999). The cellular response to p53: the decision between life and death. *Oncogene* **18**, 6145-6157. doi:10.1038/sj.onc.1203130

Storey, K. B. (1998). Survival under stress: molecular mechanisms of metabolic rate depression in animals. *S. Afr. J. Zool.* **33**, 55-64. doi:10.1080/02541858.1998.11448454

Storey, K. B. (2004). Molecular mechanisms of anoxia tolerance. *Int. Congr. Ser.* **1275**, 47-54. doi:10.1016/j.ics.2004.08.072

Storey, K. B. (2015). Regulation of hypometabolism: insights into epigenetic controls. *J. Exp. Biol.* **218**, 150-159. doi:10.1242/jeb.106369

Storey, K. B. and Storey, J. M. (1990). Metabolic rate depression and biochemical adaptation in anaerobiosis, hibernation and estivation. *Q. Rev. Biol.* **65**, 145-174. doi:10.1086/416717

Storey, K. B. and Storey, J. M. (2005). Oxygen limitation and metabolic rate depression. In *Functional Metabolism* (ed. K. B. Storey), pp. 415-442. Hoboken, NJ, USA: John Wiley & Sons, Inc.

Storey, K. B. and Storey, J. M. (2011). Heat shock proteins and hypometabolism: adaptive strategy for proteome preservation. *Res. Rep. Biol.* **2**, 57-68. doi:10.2147/RRB.S13351

Sun, S., Gu, Z., Fu, H., Zhu, J., Ge, X. and Xuan, F. (2016). Molecular cloning, characterization, and expression analysis of p53 from the oriental river prawn, *Macrobrachium nipponense*, in response to hypoxia. *Fish Shellfish Immunol.* **54**, 68-76. doi:10.1016/j.fsi.2016.03.167

Sung, Y. H., Jin, Y., Kang, Y., Devkota, S., Lee, J., Roh, J. and Lee, H.-W. (2013). Ei24, a novel E2F target gene, affects p53–independent cell death upon ultraviolet C irradiation. *J. Biol. Chem.* **288**, 31261-31267. doi:10.1074/jbc.M113.477570

Taylor, C. A. and Schuster, G. A. (2004). The crayfishes of kentucky. *Illinois Nat. Hist. Surey* **28**, 219.

Taylor, C. A., Schuster, G. A., Cooper, J. E., DiStefano, R. J., Eversole, A. G., Hamr, P., Hobbs, H. H., Robison, H. W., Skelton, C. E. and Thoma, R. F. (2007). A reassessment of the conservation status of crayfishes of the United States and Canada after 10+ years of increased awareness. *Fisheries* **32**, 372-389. doi:10.1577/1548-8446(2007)32[372:AROTCS]2.0.CO;2

Tessier, S. N., Zhang, Y., Wijenayake, S. and Storey, K. B. (2017). MAP kinase signaling and Elk1 transcriptional activity in hibernating thirteen-lined ground squirrels. *Biochim. Biophys. Acta Gen. Subj.* **1861**, 2811-2821. doi:10.1016/j.bbagen.2017.07.026

Tibbetts, R. S., Brumbaugh, K. M., Williams, J. M., Sarkaria, J. N., Cliby, W. A., Shieh, S.-Y., Taya, Y., Prives, C. and Abraham, R. T. (1999). A role for ATR in the DNA damage-induced phosphorylation of p53. *Genes Dev.* **13**, 152-157. doi:10.1101/gad.13.2.152

Weber, J. D., Taylor, L. J., Roussel, M. F., Sherr, C. J. and Bar-Sagi, D. (1999). Nucleolar Arf sequesters Mdm2 and activates p53. *Nat. Cell Biol.* **1**, 20-26. doi:10.1038/8991

Wu, D. and Prives, C. (2018). Relevance of the p53–MDM2 axis to aging. *Cell Death Differ.* **25**, 169-179. doi:10.1038/cdd.2017.187

Wu, C.-W., Tessier, S. N. and Storey, K. B. (2018). Stress-induced antioxidant defense and protein chaperone response in the freeze-tolerant wood frog *Rana sylvatica*. *Cell Stress Chaperones* **23**, 1205-1217. doi:10.1007/s12192-018-0926-x

Zhang, J. and Storey, K. B. (2016). RBioplot: an easy-to-use R pipeline for automated statistical analysis and data visualization in molecular biology and biochemistry. *PeerJ* **4**, e2436. doi:10.7717/peerj.2436

Zou, L. and Elledge, S. J. (2003). Sensing DNA damage through ATRIP recognition of RPA-ssDNA complexes. *Science* **300**, 1542-1548. doi:10.1126/science.1083430